MICROSTRUCTURE AND PROPERTIES OF MULTI-ELEMENTARY POWDERS OBTAINED BY COLD SPRAY DEPOSITION

GOUVEA Larissa A.[1], CIZEK Jan[1], JAN Vit[1], CUPERA Jan[1], DLOUHY Ivo[1]

[1] *Institute of Materials Science and Engineering - NETME Centre, Faculty of Mechanical Engineering, Brno, Czech Republic, EU, ldagouvea@gmail.com*

Abstract

The purpose of the study is to identify possible changes in different elementary powders (Al, Ti, Co, Cr, Ni, Fe) after being compacted by cold spray kinetic deposition. A deep analysis on the microstructure of the materials prior and after the deposition was performed through Scanning Electron Microscopy, Energy-Dispersive X-Ray Spectroscopy, Electron Channeling Contrast, X-ray Diffraction, Differential Scanning Calorimetry and microhardness tests.

The results indicate that there are noticeable alterations in the microstructure of the materials due to plastic deformation processes which occur during the cold spray deposition, within the material presented up to 58% increase in hardness. The bonding process is affected on cold sprayed samples depending on the chosen feedstock particles. The as-sprayed sample composition (ratio of elementary powder content) varies greatly when compared to the original one used for feedstock of pure powders. When the particles suffer heat treatment up to 750°C, solid state reactions were observed in the microstructure.

Keywords: Cold-spray; multielementary powders; solid-state reaction; diffusion-controlled reaction

1. INTRODUCTION

The Cold Gas Dynamic Spray (CS) is an innovative coating deposition technique, presenting several technological advantages over thermal spray technology, since it exploits kinetic instead of thermal energy [1]. As the deposition is accomplished at the solid state, the coating has exclusive characteristics due to the prevention of local melting, unwanted chemical reactions, suppression of tensile residual stresses [2 - 3], and its elastic properties appear to be isotropic [4]. Especially, for metallic materials or composites, high-process temperatures could increase the amount of oxides embedded in the coating and therefore reduce their performance in technical applications [5], hence the fact that, in some cases, thermal spray could not be the best choice for deposition processes.

The basic principle of the technique is that solid powders are accelerated toward a substrate over the sonic velocity, by a supersonic jet of compressed gas flowing through a de Laval nozzle. If the impact velocity exceeds a threshold value, particles undergo intensive plastic deformation and bond [6]. The temperature of the gas stream remains below the melting point of the deposited material. For a successful deposition, the geometry of the nozzle and the characteristics of the feedstock powders are essential to define the final in-flight temperature and velocity of the sprayed particles, which are strictly related to the final properties of the coating microstructure [1,8]. A very small quantity of chemical reactions or phase transformations could be triggered due to the instantaneous heat generation at the moment of impact [8].

The bonding process between the coating and the substrate and/or between the individual particles in deposition holds a great importance to the properties of the final microstructure and it could define the efficiency and quality of the deposition. Even though the literature is rich on information about the bonding process during the cold spray deposition, there are still some open questions such as the material behavior and efficiency of deposition of various kinds of particles in particle mixture under extreme deformation conditions. In this paper, several different powders were selected and mechanically mixed to prepare a coating by cold spray deposition. The as-sprayed form of the coating was compared with the elementary powders in their feedstock form and their mechanical properties were investigated, the characteristics of the deposition were evaluated and further discussed.

2. MATERIALS AND EXPERIMENTAL METHODS

Powders of Al, Co, Cr, Ti, Fe and Ni with commercial purity of 99 % were used as feedstock. The powder mixture followed a $Al_{0,2}Cr_1Co_{1.5}Ni_{1.5}Fe_1Ti_1$ stoichiometric ratio and was blended for 10 minutes to evenly distribute the individual powder grains. After this step, the blending mixture was deposited via cold gas-dynamic spray on a substrate of dimensions 100 x 60 mm, composed by austenitic stainless steel 314. The as-sprayed coating presents a thickness of approximately 350 µm, the substrate had approximately 3.5 mm of thickness. The feedstock mixture was analyzed before deposition as well as deposited on the coating. For comparison purposes, non-mixed pure powders were also matter of investigation, they were called as green sample. In order to analyze the thermal behavior of the samples, the feedstock mixture before deposition was cold-pressed in small pellets and consecutively heated up on DSC. The detailed information of all samples used in this work is described on (**Table 1**), as follows:

Table 1 Description of samples used on the study.

Name	Description	Name	Description
A2	Cold-sprayed coating.	A6	Heat Treatment via DSC. Temperature up to 750 °C.
A3	Feedstock Mixture.	A7	Heat Treatment via DSC. Temperature up to 630 °C.
A4	Cold-pressed powder for DSC.	A8	Heat Treatment via DSC. Temperature up to 560 °C.
A5	Green sample (Non-mixed powder).	A9	Heat Treatment via DSC. Temperature up to 460 °C.

The cold spray deposition was performed in a High Pressure Cold Spray System machine from Plasma Giken (Saitama, Japan) in a PCS-1000, with Laval nozzle made of Tungsten Carbide. The gas used in the chamber was Nitrogen and the pressure and temperature used were 5.0 MPa and 500 °C. Feed disk revolutions: 4 RPM; powder gas pressure 5.15 MPa and powder gas flow: 484 SLM. The nozzle stand-off distance was 30 mm and the robot-mounted gun traverse speed was 100 mm / s. The spray angle was 90°, the number of passes was only 1.

The materials characterization was done by Scanning Electron Microscope (SEM), Energy-Dispersive X-Ray Spectroscopy (EDS), Electron Channeling Contrast (ECC), X-ray Diffraction (XRD), Differential Scanning Calorimetry (DSC) and microhardness tests.

The constituent phases were analyzed based on XRD, through the diffractometer Philips X'Pert, operated under the voltage of 40 kV with current of 30 mA. A continuous scanning was performed with 2θ between 20° and 120° using a speed of 0.02° / min and step size of 0.0167°. The radiation used was Cu-Kα with λ=1.54056 Å. "PANanalytical X`Pert High Score" software was also used to compare the XRD profiles with standards compiled by the Joint Committee on Powder Diffraction and Standards (JCPDS).

Microhardness HV 0.1 was measured on the as-sprayed sample (A2), as well as on the mixed feedstock powder (A3) and on the non-mixed pure powders (A5), performing 10 different indentations on nickel particles using Leco LM 247AT microhardness tester.

The thermal behaviour of the cold pressed powders was analyzed by DSC. The experiment was performed using Setsys Evolution calorimeter from Setaram. The cold pressed sample was placed in a crucible and heated in dynamic argon atmosphere up to 750 °C at a rate of 10 K / min.

3. RESULTS AND DISCUSSION

The microstructure of the as sprayed coating produced by CS can be seen in (**Figure 1a**). Its EDS map shows the distribution of the elements after the deposition. The particles which are closer to the coating / substrate interface experienced considerable more deformation than on the top of the coating due to the successive impact of the particles during deposition. It's clear that the elements deposited are completely separated and did not react with each other after the CS deposition. The elements are isolated and the dimensions of the deformed grains were of from 20 up to 60 µm, approximately. The average size of feedstock powders is: Co - 2.5 µm; Fe - 4 µm; Ti - 30 µm; Cr - 35 µm; Al - 55 µm; Ni - 60 µm.

It can be noticed that due to the high impact of CS deposition, some of the elements - i.e. Co and Fe - have agglomerated and formed bigger grains, as showed in (**Figure 1b**), which cobalt agglomerated up to 25 µm.

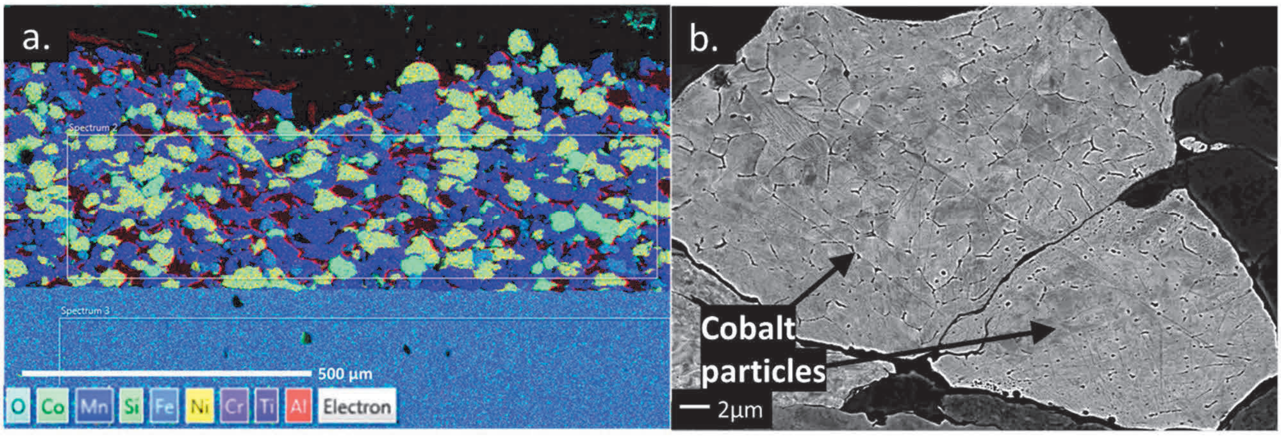

Figure 1 a) EDS Mapping of as-sprayed coating;
b) Micrograph of cobalt agglomeration in as-sprayed coating

The theoretical composition of the feedstock powder varies greatly from the one as-sprayed (**Table 2**). This phenomenon occurs because distinct materials have different suitability for CS method.

Table 2 Differences in composition of feedstock powders and as-sprayed sample

Element	Feedstock composition [at. %]	As-sprayed - Average Composition [at. %]	Standard Error (+-)
Al	3.23	29.32	0.80
Co	24.19	6.18	0.57
Cr	16.13	12.26	0.43
Fe	16.13	4.95	0.12
Ni	24.19	17.25	0.29
Ti	16.13	30.05	0.47

The suitability of the material depends on their deformation properties, so materials with relatively low melting point and low mechanical strength such as Al are ideal materials, exhibiting low yield strength and softening at elevated temperatures [1, 9]. Materials with higher strength such as Fe and Ni, the low process temperatures normally do not provide enough energy for successful deposition, even though they could still be used for Cold Spray technology [1, 10]. For that reason, the deposition efficiency is different depending on the element used. The amount of aluminum successfully deposited was much higher [(29.3 ± 0.8) at %] than the starting composition (3.3 at%) and the same phenomenon happened to titanium [(30.1 ± 0.5) at %], while its theoretical composition was supposed to be 16.1 at%, even though it has high mechanical strength and high melting point, suggesting that the used parameters were closer to the optimum ones for the deposition of titanium particles, leading to reduction in the content of the other particles, such as Ni, Fe, Co and Cr. In literature, there are several successful titanium depositions when the parameters are rightly chosen [11, 12]. The other elements didn't adhere as well and their as-sprayed composition is much less than it was first intended to be.

XRD characterization was performed on the as-sprayed sample and feedstock powder (**Figure 2**).

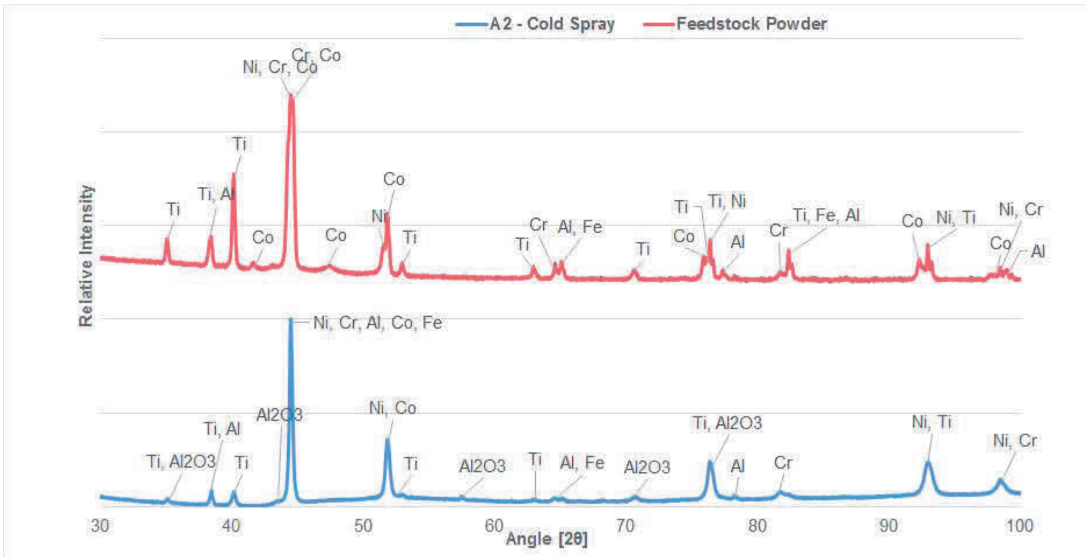

Figure 2 XRD patterns of feedstock powder and cold-sprayed coating

Aside from the peaks pertaining to the individual pure metallic elements, no peaks of other phases were observed in the measured XRD spectra of the as-sprayed sample, except for Al2O3. The difference on the intensity of the peaks was probably caused due to the difference in ratio of the elements, since the feedstock composition changed with the deposition. There is a widening of the 2θ peaks on 76°, 93° and 98°, which indicates plastic deformation of the as-sprayed sample due to lattice distortion.

The Microhardness tests were performed on Nickel particles under 100g load. (**Table 3**) shows the results.

Table 3 Average microhardness results performed on Nickel particles under 100g load

Name	Average results - Vickers [HV]	Standard Error (+-)
Non-mixed powder (A5)	104.1	3.4
Feedstock mixture (A3)	120.6	6.0
Cold-sprayed coating (A2)	164.4	5.4

The results exhibit an increase of the hardness level. The non-mixed sample exhibits the lowest hardness values (HV104.1±3.4), while after blending the powders for 10 minutes caused an increase of the average hardness level of 16 % (HV120.6±6.0). Due to the high velocity impact on deposition and work-hardening, the material experienced severe plastic deformation, the as-sprayed sample presented 58 % higher values of average hardness (HV164.4±5.4).

The material suffered strong plastic deformation and formed subgrains after CS deposition (**Figure 3**) for all elements. In (**Figure 3c**), it is noticeable that due to the high-pressure generation at the moment of impact, finer microstructures can be seen close to the grain boundaries, while in its middle, there are coarser grains. It is important to point out the difference between deformation levels in the particles closer to the interface of the coating/substrate and those on the top of the coating. As it can be seen in (**Figure 3b, 3c, 3e and 3f**) respectively, the material suffered much higher plastic deformation on the region close to the interface.

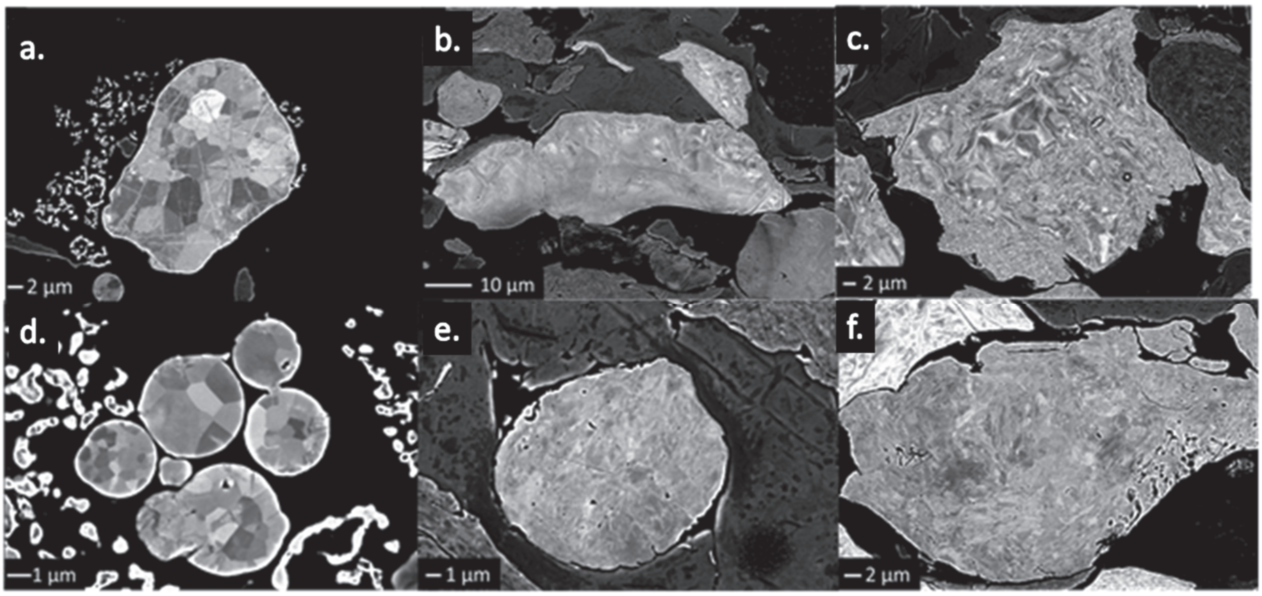

Figure 3 Electron Channeling Contrast Images: a) Ni on non-mixed green sample; b) As-sprayed Ni close to the top of the coating; c) As-sprayed Ni close to the interface; d) Fe on green sample; e) As-sprayed Fe close to the top of the coating; f) As-sprayed Fe close to the interface

The thermal behavior of the feedstock powders was analyzed in order to observe possible phases that could be formed during heat treatments following the cold spray deposition. Different measurements on temperatures from 460 °C, 560 °C, 630 °C up to 750 °C were reached to see the evolution of the microstructure in higher temperatures range than used in CS technique.

There are only exothermic reactions present on the DSC curves (**Figure 4**), which might suggest that, at 438, 535 and 634 °C peaks, the material has experienced phase changes in solid state. At 660 °C, Al probably reacted immediately with other elements after its melting. In different temperatures, the particles have different surroundings, as in **Figure 4b**, which shows what the microstructure looks like in the highest temperature. At 460 °C, the only present reaction is between Co particles and Fe. At 560 °C, Ni reacts with Fe and small portion of Co, as well as Ti particles reacted with Ni, Co and Fe. On the other hand, at 630 °C, besides all the latest reactions, Co particles form phases with Al, Fe and Ti, as well as Fe particles react with Ni, Co and Ti. At last, on 750 °C, it is possible to observe many reactions amongst the elements, with diffusivity of Fe, Co and Ti into Ni, as well as Al particles with Fe, Co and Ti.

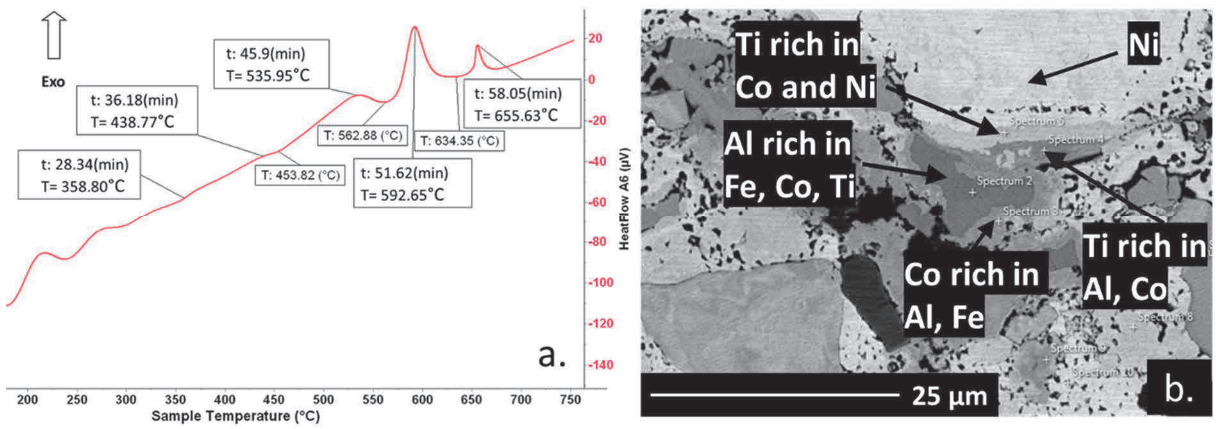

Figure 4 a) DSC curve analysis of feedstock powders up to 750°C;
b) Microstructure of A6 - heat treatment at 750°C

4. CONCLUSION

The cold spray deposition does not show any reaction amongst Al, Ti, Ni, Fe, Cr and Co elements, except for aluminum oxidation. The technique showed limitations in some extent on the deposition efficiency. The sticking coefficient is diverse depending on the element used, therefore the efficiency of Co, Fe and Ni was much lower than expected, although Al and Ti have great efficiency on deposition on stainless steels 314 substrates. The average hardness level of Ni particles increased by 58 % with the cold spray. All elements presented strong plastic deformation and formation of subgrains after the deposition. On DSC curves, from 460 °C, 560 °C, 630 °C up to 750 °C, solid state reactions are observed and distinct phases are formed due to the diffusivity of different elements into elementary powders. The main reaction observed was diffusion of Fe and Co into Ni particles.

ACKNOWLEDGEMENTS

This research has been supported by the research project no. Lo1202, within NETME Centre Plus, project of Ministry of Education, Youth and Sports under the "National Sustainability Programme".

REFERENCES

[1] MORIDI, A., HASSANI-GANGARAJ, S.M., GUAGLIANO, M., et al. Cold Spray coating: review of material systems and future perspectives, Surface Engineering, 2014, vol. 36, no. 6, pp. 369-395.

[2] KOSAREV, V.F., KLINKOV, S.V., ALKHIMOV, A.P., et al. On Some Aspects of Gas Dynamics of the Cold Spray Process, Journal of Thermal Spray Technology, 2003, vol. 12, no. 2, pp. 265-281.

[3] HUSSAIN, T., MCCARTNEY, D.G., SHIPWAY, P.H., et al. Corrosion Behavior of Cold Sprayed Titanium Coatings and Free Standing Deposit, Journal of Thermal Spray Technology, 2011, vol. 20, no. 1-2, pp. 260-274.

[4] SEINER, H., CIZEK, J., SEDLAK, P., HUANG, R., CUPERA, J., DLOUHY, I., LANDA, M. Elastic moduli and elastic anisotropy of cold sprayed metallic coatings, Surface & Coatings Technology, 2016, Vol. 291, 342-347.

[5] GARTNER, F., STOLTENHOFF, T., SCHMIDT, T., et al. The Cold Spray Process and Its potential for Industrial Applications, Journal of Thermal Spray Technology, 2006, vol. 15, no. 2, pp. 223.

[6] DYKHUIZEN, R.C., SMITH, M.F. Gas Dynamic Principles of Cold Spray, Journal of Thermal Spray Technology, 1998, vol. 7, issue 2, pp. 205-212.

[7] LIMA, R.S., KUCUK, A., BERNDT, C.C. Deposition efficiency, mechanical properties and coating roughness in cold-sprayed titanium, Journal of Materials Science Letters, 2002, vol. 21, pp. 1687-1689.

[8] LEE, C., KIM, J. Microstructure of Kinetic Spray Coatings: A Review, Journal of Thermal Spray Technology, 2015, vol. 24, no. 4, pp. 592-610.

[9] WANG, Q., BIRBILIS, N., ZHANG, M. X. On the formation of a diffusion bond from cold-spray coatings, Metallurgical and Materials Transactions A: Phys. Metall. Mater. Sci., 2012, vol. 43, pp. 1395-1399.

[10] XIONG, Y., BAE, G. Bae, XIONG, X. et al. The effects of successive impacts and cold welds on the deposition onset of cold spray coatings, Journal of Thermal Spray Technology, 2010, vol. 19, pp. 575-585.

[11] SHUKLA, V., ELLIOT, G.S., KEAR, B.H., et al. Hyperkinetic deposition of nanopowders by supersonic rectangular jet impingement, Scripta Materialia, 2001, vol. 44, no. 8-9, pp. 2179-2182.

[12] PRICE, T. S., SHIPWAY, P. H., MCCARTNEY, D. G. Effect of cold spray deposition of a titanium coating on fatigue behavior of a titanium alloy, Journal of Thermal Spray Technology, 2006, vol. 15, no. 4, pp. 507-512.